

Moreover, the measurement agrees well with the simulation, verifying the proposed design concept.

## REFERENCES

1. X. Guan, Z. Ma, P. Cai, Y. Kobayashi, T. Anada, and G. Hagiwara, Synthesis of dual-band bandpass filters using successive frequency transformations and circuit conversions, *IEEE Microwave Wireless Compon Lett* 16 (2006).
2. H.J. Lin, X.W. Shi, X.H. Wang, C.L. Li, and Q. Li, A novel CPW dual passband filter using the split-modes of loaded stub square loop resonators, *Prog Electromagn Res Lett* 16, 2010.
3. C.F. Chen, T.Y. Huang, and R.B. Wu, Design of dual- and tri passband filters using alternately cascaded multiband resonators, *IEEE Trans Microwave Theory Tech* 54, 2006.
4. M.H. Weng, H.W. Wu, and Y.K. Su, Compact and low loss dual-band bandpass filter using pseudo-interdigital stepped impedance resonators for WLANs, *IEEE Microwave Wireless Compon Lett* 17, 2007.
5. Y.C. Chang, C.H. Kao, M.H. Weng, and R.Y. Yang, A novel compact dual-band bandpass filter using asymmetric SIRs for WLANs, *Microwave Opt Technol Lett* 50, 2008.
6. M.H. Weng, H.W. Wu, K. Shu, R.Y. Yang, and Y.K. Su, A novel tri-band bandpass filter using multilayer-based substrates for WiMAX, *European Microwave Conference (EuMC)*, Munich, Germany, 2007.
7. IE3D Simulator, Zeland Software, Inc., Fremont, CA, 2002.
8. Y.C. Chang, C.H. Kao, M.H. Weng, and R.Y. Yang, Design of the compact wideband bandpass filter with low loss, high selectivity and wide stopband, *IEEE Microwave Wireless Compon Lett* 18, 2008.
9. G.L. Matthaei, L. Young, and E.M.T. Jones, *Microwave filters, impedance-matching networks, and coupling structures*. McGraw-Hill, New York.
10. J.S. Hong and M.J. Lancaster, *Microstrip filter for RF/microwave application*. Wiley, New York, 2001.

© 2011 Wiley Periodicals, Inc.

## A SMALL-SIZE PENTABAND HAND-SHAPED COPLANAR WAVEGUIDE-FED MONOPOLE ANTENNA

Alireza Mallahzadeh, Ali Foudazi, and Sajad Mohammad Ali Nezhad

Shahed University, Persian Gulf Highway, Tehran, Islamic Republic of Iran; Corresponding author: alinezhad@shahed.ac.ir

Received 29 September 2010

**ABSTRACT:** A novel small-size simple structure pentaband coplanar waveguide (CPW) fed monopole antenna is presented. The antenna configuration is composed of several narrow strips that are connected to a 50-ohm CPW feed line. The length of each strip, which acting as resonance path, is  $\lambda/4$  at operating frequencies. The antenna is designed to operate over the worldwide interoperability for microwave access and wireless local area networks frequency bands of 2.4, 3.3, 3.7, 5.2, and 5.8 GHz. It was found that the results of simulation and measurement agree well over each separated frequency bands.

© 2011 Wiley Periodicals, Inc. *Microwave Opt Technol Lett* 53:1576–1579, 2011; View this article online at [wileyonlinelibrary.com](http://wileyonlinelibrary.com). DOI 10.1002/mop.26025

**Key words:** monopole antenna; CPW-fed; pentaband

## 1. INTRODUCTION

In recent decade, wireless local area networks (WLAN) and worldwide interoperability for microwave access (WiMAX) have evolved at very high rate for modern communication sys-

tems. Thus, design an antenna that can operate at WLAN and WiMAX frequency bands have increasingly demanded.

Different studies were paid attention on planar antennas that were designed to operate at WLAN and WiMAX frequency bands. In comparison to nonprinted antennas, printed antennas due to their small size, low profile, lightweight, and low cost are more attractive [1]. Among different structure of printed antennas, printed coplanar waveguide (CPW)-fed antenna is more appropriate for WLAN and WiMAX applications, due to its omnidirectional radiation coverage, little dependence of the characteristic impedance on substrate height, single metallic layer structure, easy integration to monolithic microwave integrated circuits, and comparatively higher bandwidth [2, 3].

Recently, there has been an increase in the use of antenna operating at several frequency bands for WLAN and WiMAX systems. Several techniques to obtain multiband CPW antenna were reported in literatures. One of the techniques is the design of a wideband antenna and introducing notches to obtain the multiband behavior [4]. In the second technique, by creating multi-independent resonance paths, multiband CPW antenna is obtained. A dual-band CPW-fed closed rectangular ring monopole antenna with a vertical strip [5], a triple-band CPW-fed F-shaped monopole antenna [6], and a dual-frequency double inverted-L CPW-fed monopole antenna [7] were reported. In the third technique, by inserting parasitic elements near or behind the radiating element, multiband CPW antenna can be achieved [8].

According to literature review of CPW antenna so far, designed multiband CPW antennas are capable to operate as quad-band antenna. Also, designed multiband CPW antennas by

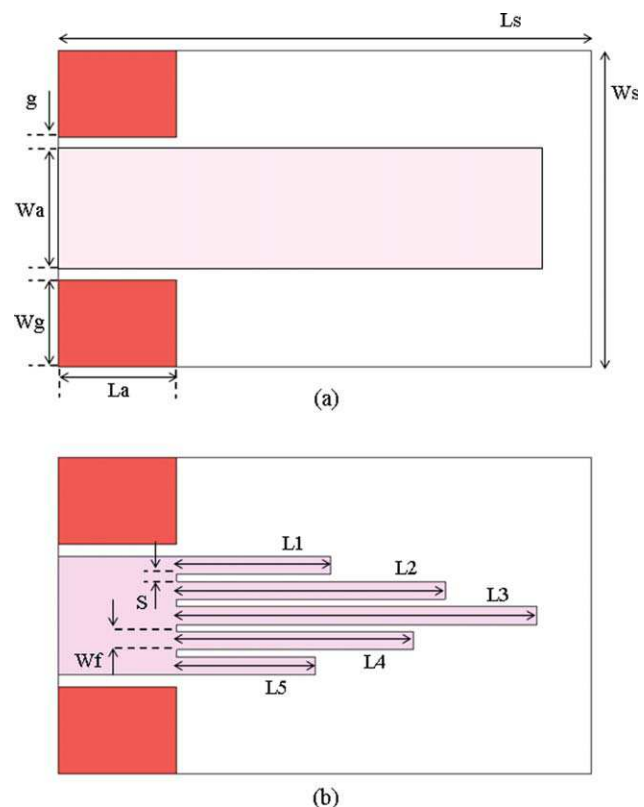


**Figure 1** The configuration of proposed multiband antenna: (a) single resonance patch and (b) pentaband antenna. [Color figure can be viewed in the online issue, which is available at [wileyonlinelibrary.com](http://wileyonlinelibrary.com)]

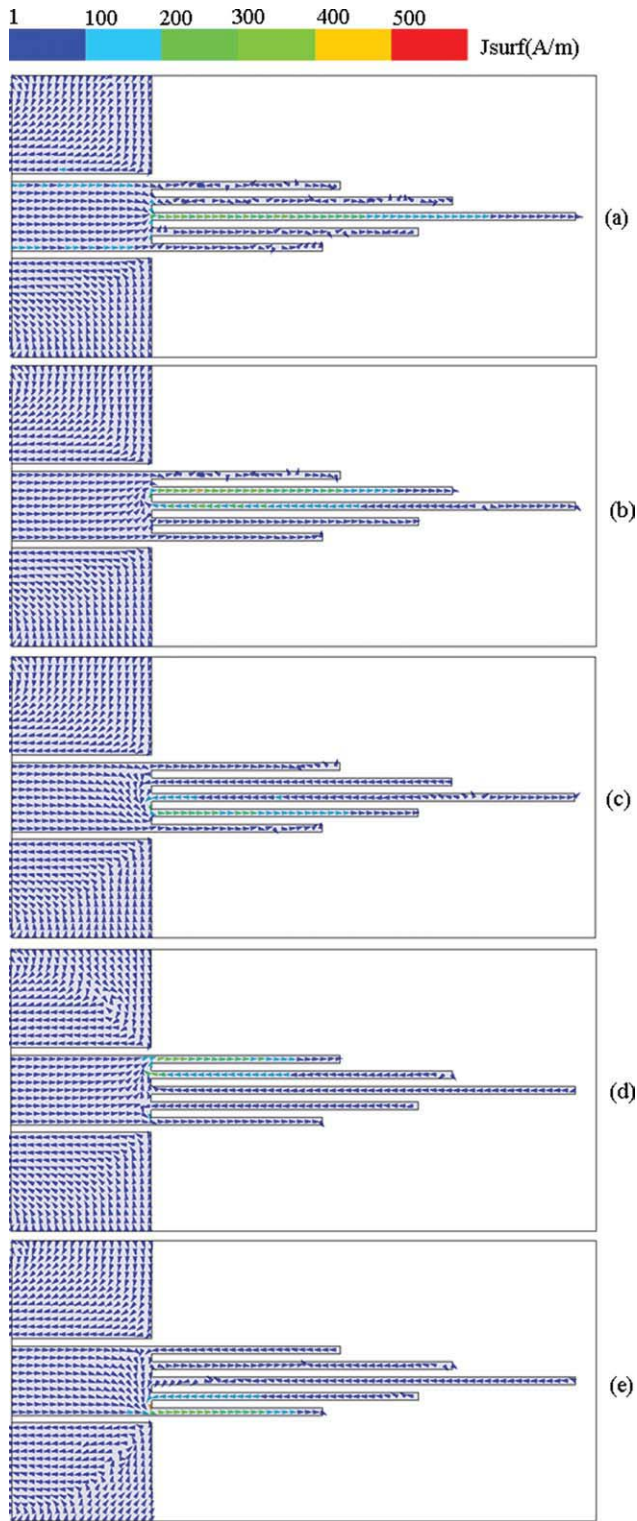


**Figure 2** Current distribution of pentaband antenna at various frequencies of (a) 2.4, (b) 3.3, (c) 3.7, (d) 5.2, and (e) 5.8 GHz. [Color figure can be viewed in the online issue, which is available at [wileyonlinelibrary.com](http://wileyonlinelibrary.com)]

different methods have complicated structures and large dimensions.

In this letter, a simple printed antenna is presented. The proposed CPW-fed antenna is considered to operate as a pentaband antenna that covers WLAN/WiMAX frequency bands. The antenna is small-size at both electrical and physical dimensions.

The proposed multiband antenna is simulated and pentaband one is fabricated and measured.

## 2. ANTENNA DESIGN

A simple base radiating CPW-fed antenna is shown in Figure 1(a). The simple structure of CPW-fed antenna is composed of a quarter-wavelength long resonant strip with the same width as feed line, which connected to the feed line, and two rectangular separated ground planes at two sides and no metallization on the back side of substrate. The dimension of antenna is very compact with the substrate area of  $12 \times 22 \text{ mm}^2$ , which is constructed on a 1 mm thick FR4 with  $\epsilon_r = 4.4$  and loss tangent 0.02. The width of feed line is fixed at 5 mm and gap spacing of 0.3 mm to achieve 50 ohm characteristic impedance. The length of feed line is set to 8 mm as well as the length of ground planes.

To obtain a multiband monopole antenna, one can use several single resonant paths that produce separated resonance behaviors. To accomplish this, the resonant paths should be a multiplication of  $\lambda_g/4$  at desired frequencies. The base CPW-fed antenna of Figure 1(a) is designed to operate on lower frequency band of 2.4 GHz for WLAN/WiMAX systems. As shown in Figure 1(b), to obtain multiband behaviors on the base antenna, the base radiating patch can be divided into several narrow paths by inserting some rectangular narrow slits in the middle part of the base antenna. Thus, to achieve N-band behavior, one should insert N-1 slits in the base radiating patch. By changing the length of created arms, which are connected to the feed line, each arm is capable to operate as a single resonant frequency. The length of the paths can be set to the value of  $\lambda_g/4$  for desired higher resonance bands and are independent of the length of other arms. Therefore, the dimension of pentaband CPW-fed antenna and the base CPW-fed antenna is small size. Also, the dimension of developed pentaband antenna is electrically small sized. The electrical size of the antenna is approximately  $0.14 \lambda_g \times 0.3 \lambda_g$  in terms of the desired lowest operating frequency of 2.4 GHz.

The resonance frequencies of developed pentaband CPW-fed antenna can be easily obtained by:

$$L_n = \lambda_{gn}/4, \quad n = 1 \text{ to } 5$$

The optimal antenna parameters for the pentaband behaviors at 2.4, 3.3, 3.7, 5.2, and 5.8 GHz are set as follows:  $W_a = 3$ ,  $g = 0.3$ ,  $W_g = 4.2$ ,  $L_a = 6$ ,  $W_f = 0.35$ ,  $L_1 = 8.05$ ,  $L_2 = 12.85$ ,  $L_3 = 18.1$ ,  $L_4 = 11.4$ ,  $L_5 = 7.3 \text{ mm}$ .

The current distribution of pentaband antenna on the radiating patch is presented for better understanding of the behavior of

**TABLE 1** Total Length of Strips to Design Multiband Antenna

Resonance Frequency (GHz)	L1 (mm)	L2 (mm)	L3 (mm)	L4 (mm)
2.4	18	Remove	Remove	Remove
3.3	13.25	Remove	Remove	Remove
5.2	18	Remove	Remove	Remove
2.4 and 3.3	18	13.25	Remove	Remove
2.4 and 5.2	18	8	Remove	Remove
3.3 and 5.2	13.25	8	Remove	Remove
2.4, 3.3, and 5.2	18	13.25	8	Remove
2.4, 3.7, and 5.2	18	10.75	8	Remove
2.4, 5.2, and 5.8	18	8	7.25	Remove
2.4, 3.3, 5.2, and 5.8	18	12.5	8	7.25

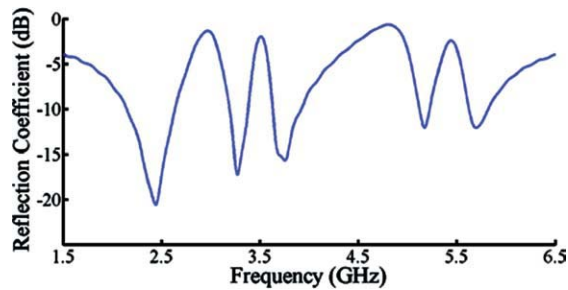


**Figure 3** Measured reflection coefficient of pentaband antenna. [Color figure can be viewed in the online issue, which is available at [wileyonlinelibrary.com](http://wileyonlinelibrary.com)]

pentaband CPW-fed monopole antenna. The surface current distributions, as obtained through HFSS package, at frequencies of 2.4, 3.3, 3.7, 5.2, and 5.8 GHz are given in Figures 2(a)–2(e), respectively. As seen in this figure, by changing the resonance frequency, the relevant arm is activated in each resonance,

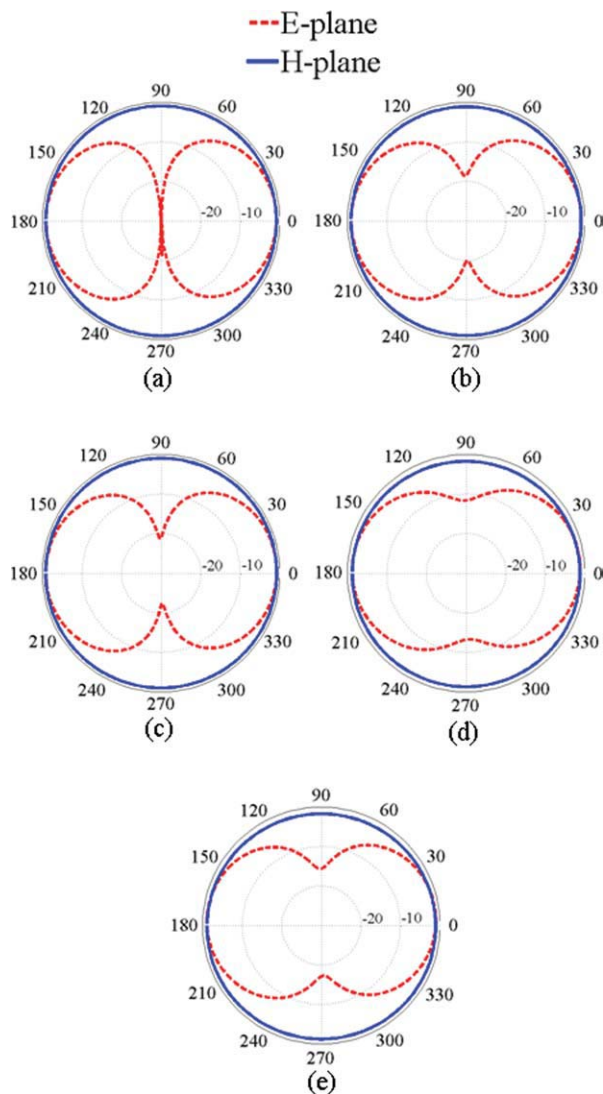


**Figure 4** E-plane and H-plane radiation pattern of the pentaband antenna at various frequencies of (a) 2.4, (b) 3.3, (c) 3.7, (d) 5.2, and (e) 5.8 GHz. [Color figure can be viewed in the online issue, which is available at [wileyonlinelibrary.com](http://wileyonlinelibrary.com)]

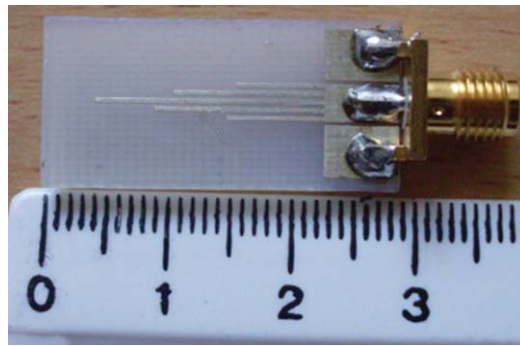


**Figure 5** Fabricated pentaband antenna. [Color figure can be viewed in the online issue, which is available at [wileyonlinelibrary.com](http://wileyonlinelibrary.com)]

whereas the other arms become inactive due to their negligible current. Moreover, the current distribution on each activated arm shows the maximum current at the beginning of the path and minimum current at the end of path, and proves that each arm independently passes current distribution with  $\lambda/4$  length in resonance.

Table 1 shows some different resonance frequencies that could be achieved using this antenna. Depending on number of desired resonance frequencies, the same numbers of resonant paths are used in this table. It is obvious that the multiband antenna can produce all WiMAX/WLAN frequencies of 2.4–5.8 GHz.

### 3. RESULT AND DISCUSSION

The pentaband CPW-fed monopole antenna was fabricated and tested. To obtain any number of multiband antennas, different separated paths are set to the length of quarter wavelength at desired resonance frequencies. Figure 3 shows the simulated and measured reflection coefficient results of proposed pentaband antenna. The simulated and experimentally measured results show good agreement. The results show that the proposed antenna has impedance bandwidth of 2.275–2.53, 3.23–3.4, 3.6–3.75, 5.15–5.34, and 5.75–5.97 GHz with appropriate reflection coefficient below  $-10$  dB.

The measured E-plane and H-plane radiation patterns of the proposed antenna at 2.4, 3.3, 3.7, 5.2, and 5.8 GHz are shown in Figure 4. Also, both copolar and crosspolar components are presented, which show good radiation characteristic over pentaband resonance. It should be noticed that the omnidirectional H-plane pattern varies within  $\pm 1$  dB throughout the WLAN and WiMAX frequencies. Moreover, the E-plane pattern is very stable with changes in frequency. Because of good radiation patterns and appropriate reflection coefficient, the fabricated pentaband hand-shaped antenna as shown in Figure 5 is suitable to use for WLAN and WiMAX systems.

### 4. CONCLUSION

A hand-shaped CPW-fed antenna that covers the WLAN and WiMAX frequency bands is presented. By using the method of inserting quarter-wavelength long paths on a base radiating patch, multiband antenna is obtained with finely tuning characteristic. The small-size fabricated antenna shows a stable and omnidirectional radiation patterns across all bands.

### REFERENCES

1. C.-C. Lin, S.-W. Kuo, and H.-R. Chuang, A 2.4-GHz printed meander line antenna for USB WLAN with notebook-PC housing, *IEEE Microw Wirel Compon Lett*, 15 (2005), 546–548.

2. P.C. Bybi, G. Augustin, B. Jitha, C.K. Aanandan, K. Vasudevan, and P. Mohanan, A quasi-omnidirectional antenna for modern wireless communication gadgets, *IEEE Antennas Wirel Propag Lett*, 7 (2008), 505–508.
3. R. Sujith, S. Mridula, P. Binu, D. Laila, R. Dinesh, and P. Mohanan, Compact CPW-fed ground effected H-shaped slot antenna with harmonic suppression and stable radiation characteristics, *Electron Lett*, 46 (2010).
4. H.-W. Liu, C.-H. Ku, and C.-F. Yang, Novel CPW-Fed planar monopole antenna for WiMAX/WLAN applications, *IEEE Antennas Wirel Propag Lett* 9 (2010), 240–243.
5. L. Zhang, Y.-C. Jiao, G. Zhao, Y. Song, and F.-S. Zhang, Broad-band dual-band CPW-fed closed rectangular ring monopole antenna with a vertical strip for WLAN operation, *Microw Opt Technol Lett*, 50 (2008), 1929–1931.
6. Y. Jee and Y.-M. Seo, Triple-band CPW-fed compact monopole antennas for GSM/PCS/DCS/WCDMA applications, *Electron Lett* 45 (2009).
7. S. Chaimool and K.L. Chung, CPW-fed mirrored-L monopole antenna with distinct triple bands for WiFi and WiMAX applications, *Electron Lett* 45 (2009).
8. S. Hong, K. Chung, J. Kim, and J. Choi, Design of quad-band antenna for wireless communication, *Microw Opt Technol Lett* 51 (2009), 2277–2281.

© 2011 Wiley Periodicals, Inc.

## COST-EFFECTIVE ALL-SEMICONDUCTOR $4 \times 40$ GBIT/S TRANSMISSION IN THE 1310-NM WAVELENGTH DOMAIN

Jaroslaw Turkiewicz\*

Electro-Optical Communications Group, Eindhoven University of Technology, Eindhoven, The Netherlands; Corresponding author: jturkiew@tele.pw.edu.pl

Received 29 September 2010

**ABSTRACT:** Error-free transmission of  $4 \times 40$  Gbit/s over 50 km of standard single mode fiber in the 1310-nm wavelength domain is demonstrated. The obtained results prove applicability of the 1310-nm wavelength domain to support the cost-effective medium range high capacity transmission systems, e.g., future 400 Gbit/s Ethernet standard. © 2011 Wiley Periodicals, Inc. *Microwave Opt Technol Lett* 53:1579–1582, 2011; View this article online at [wileyonlinelibrary.com](http://wileyonlinelibrary.com). DOI 10.1002/mop.26065

**Key words:** optical communications; semiconductor optical amplifier; optical fiber; wavelength division multiplexing

### 1. INTRODUCTION

The ever growing number of Internet users and bandwidth hungry application is forcing telecommunication operators to constantly upgrade network infrastructure. Therefore, new transmission techniques are needed to fulfill bandwidth demand. Generally speaking, one 10 Gbit/s transmission link can support ten thousand 1 Mbit/s users (1 Mbit/s is a typical transmission rate in current xDSL-based access systems). However, with the foreseen in 2015 [1] roll out of access systems with 1 Gbit/s per user, one 100 Gbit/s channel will server only 100 users. This dramatically changes economy of optical transmission and forces to look for cost-effective solutions in terms of investment as well as operational cost.

\*Present address: Institute of Telecommunications, Warsaw University of Technology, ul. Nowowiejska 15/19, Warsaw, Poland

Significant effort is devoted to the techniques that increase the transmission speed in a single wavelength channel. Advanced modulation formats techniques have been developed to realize transmission of 100 Gbit/s and more in one channel [2], which gives enormous capacity in combination with dense wavelength division multiplexing (DWDM). Those systems start to be commercially available [3, 4]. Using optical time domain multiplexing (OTDM), even higher bit rates have been demonstrated [5], but still OTDM transmission is far from being soon commercialized. The other approach to increase the transmission capacity of the optical fiber that gets significantly less attention is based on usage of other than the 1550-nm transmission window.

The 1310-nm transmission window is characterized by relatively low attenuation of about 0.4 dB/km and low dispersion value for standard single mode fiber (SSMF) the most installed fiber nowadays. This results in virtual absence of dispersion related signal distortions for bit rates up to 40 Gbit/s over distances to 50 km. Moreover, the 1310-nm wavelength domain can be used in parallel to the 1550-nm transmission window. Current applications of the 1310-nm wavelength domain are limited to up-stream channel in passive optical networks transmission as well as a newly developed IEEE 802.3ba Ethernet standard [6]. IEEE 802.3ba (100 Gbit Ethernet) standardizes transmission of  $4 \times 25$  Gbit/s over 40 km of SSMF.

In this article, all-semiconductor DWDM  $4 \times 40$  Gbit/s over 50 km of SSMF transmission in the 1310-nm wavelength domain is demonstrated in detail, showing that the 1310-nm transmission window is a serious candidate to support the needs of telecommunication network operators and their customers. Exclusively, all-semiconductor components are used like semiconductor optical amplifiers (SOA) and electro-absorption modulators, which gives very good prospect for significant cost savings and integration. The proposed solution forms a basis for cost-effective transmission of 400 Gbit/s, e.g., for the future Ethernet standards.

Previously presented experiments in the 1310-nm wavelength domain included  $4 \times 20$  Gbit/s DWDM over 90 km of SSMF [7],  $4 \times 10$  Gbit/s DWDM over 200 km of SSMF [8], and  $4 \times 25$  Gbit/s DWDM over 50 km of SSMF [9]. An interesting experiment was presented in Ref. 10, where unrepeated  $8 \times 10$  Gbit/s transmission over 141 km SSMF is presented. However, it required two complicated and expensive Raman amplifiers, which are far from being cost-effective in such applications. Therefore, to the best of author's knowledge the presented results are the highest reported transmission capacity in the 1310-nm wavelength domain.

### 2. EXPERIMENTAL SETUP

Figure 1 shows the experimental setup. The  $4 \times 40$  Gbit/s DWDM transmitter consisted of four continuous wave (CW) lasers at wavelengths: 1311.5, 1312.9, 1317.0, and 1319.8 nm (Channels 1–4, respectively). The unequal channel allocation scheme was applied to eliminate the FWM related penalty due to the high input power to the transmission fiber. All four CW signals were combined in a following AWG. The average AWG insertion loss was 3.2 dB and the polarization dependent loss was about 1 dB. In the EAM, all signals were modulated simultaneously at the bit rate 40 Gbit/s with the PRBS of length  $2^{31}-1$  coming from pattern generator. The measured static extinction ratio of the EAM for the voltage swing of 3 Vpp was 12 dB. The used EAM was a commercially available device. To decorrelate the bit patterns a 2.5-km long dispersion shifted fiber (DSF) was used. The DSF had the absolute dispersion value of 42.5 ps/nm. Application of a 5-km long DSF led to signal distortions due to accumulated dispersion. To compensate for